BEM computations of a finite-length acoustic horn and comparison with experiment

T. H. Hodgson[a],.R. L. Underwood[b]
[a]*Department of Mechanical & Aerospace Engineering, North Carolina State University, Raleigh, NC 27695, USA*
EMail: thodgson@eos.ncsu.edu
[b]*IBM, Research Triangle Park, NC 27709, USA*
EMail: ron_underwood@vnet.ibm.com

Abstract

Classical horn theory calculates the throat impedance to predict the performance of a finite length horn by using the exit boundary condition that the impedance there is that of a rigid piston in an infinite baffle. Historically such calculations have not seemed to produce good correlation between the radiated pressure response in the far-field and the calculated throat impedance. In this re-examination of horn theory, the throat impedance is calculated for a finite three-dimensional exponentially-flared horn by the Boundary Element Method representing the horn boundaries by planar elements. The calculated impedance, for the without and with finite-baffle cases, is compared with the classical theory and computed far-field response. The computed results are also compared with a novel measurement technique for measuring the throat acoustic impedance using a fiber-optic probe for determining the loudspeaker driver motion. It is shown that there is excellent correlation between the frequency peaks in the far-field pressure and the throat impedance both for the BEM calculations and for the experimental measurements.

1 Introduction

When a sound wave passes through a tube with a small throat and exits from a large mouth, it experiences amplification of the acoustic pressure over that achieved with no horn. In view of the simple-looking physics of acoustic horn action it is, at first, surprising to find that the literature on this topic is very large. This can be partially explained by reading Lord Rayleigh's famous work "Theory of Sound" [1] (1878). There he stated "when the section of a pipe is variable, the

problem of the vibrations of air within it cannot be generally solved." The acoustic horn as used in musical reproduction and public address systems is designed to produce a smooth wave propagation in the horn, trying to create the maximum loading resistance for the vibrating loudspeaker diaphragm at the throat to work against, with a wide frequency range so that as much of the input energy is radiated as sound as is possible, usually 40-50%. This resistance (pressure p divided by velocity u) is equal to 415 Rayls in SI units for air at standard atmospheric conditions. Figure 1 shows the real and imaginary impedance vs frequency for an infinite length exponential horn with area $A=A_0e^{mx}$. Note that below the so-called cut-off frequency, $f_0=mc/(2\pi)$, propagation cannot occur, the diaphragm producing "sloshing" or reactive motion.

Many of the great eighteenth and nineteenth century mathematicians studied equations for wave motion in pipes. But it seems the most often quoted description for a horn was given by Webster [2] (1919) who assumed that the sound wavefronts in the horn were planar (incorrect) and then derived a one-dimensional equation now named after him. He deduced that an optimum horn contour shape for a smooth throat impedance was obtained with the exponential area distribution. Much interest has been generated by this one-dimensional equation even in modern times; see Holland, Fahy, and Morfey [3] for an extensive review and analysis using this equation. Their method could not predict the far-field pressure.

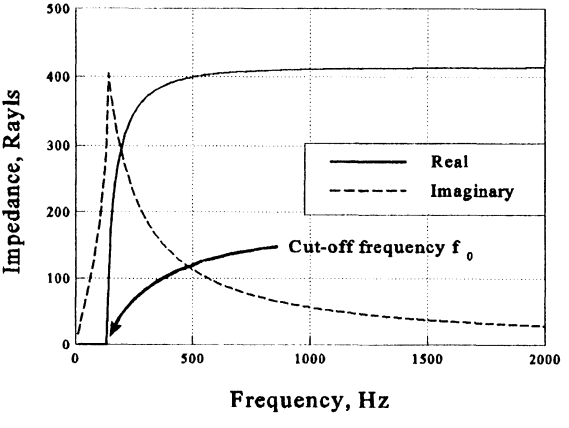

Figure 1 Acoustical resistance and reactance of an exponential horn of infinite length, flare rate m=5.

But, of course, the wave propagation along a finite horn and the exiting of the sound waves into free space is really a far more complicated wave propagation problem, involving the boundary conditions at exit, diffraction of the waves at exit, and the reflection of the effects of the exit boundary conditions back to the throat. Exponential horns seem to give the smoothest throat impedance result with an infinite baffle, although near cut-off there is a group velocity effect that could lead to waveform distortion. The text most often quoted on horn acoustics is by Olson [4] (1940). Here the scalar wave equation is solved for a circular cross-section with the boundary conditions at the exit taken as the

impedance of a circular opening or piston in an infinite baffle. It is the Olson curves of throat impedance vs frequency that are usually quoted in the literature. A further application of this method for rectangular horns was made by Sauter and Soroka [5]. More details of the Struve functions used by them are given by Underwood [6]. Clearly, neither of these results can be completely correct for a horn of finite length, either without or with a finite-sized baffle.

The impetus for this research came from observing the apparent disagreement that seems to have occurred time and again between apparently reasonably smooth calculated throat impedances as a function of frequency by the Olson method and the totally dissimilar measurements of the radiated far-field pressure on axis. In many cases, peaks in the throat impedance do not seem to match peaks in the far-field pressures. A very good example of this occurrence is described by Edgar [7], see one example in Figure 2.

It would seem that a re-examination of classical horn theory, particularly finite-length horns with finite-sized baffles is warranted. Here calculation and measurement of both the throat impedance and the far-field pressure for a Klipsch K400 mid-range horn of exponential shape, f_0=400Hz, is undertaken. The BEM computations used the SYSNOISE Rev 5.2 software package compatible with an IBM RS/6000 work-station with 100MB of memory. In this method, the horn boundaries were discretized into planar element meshes and were interfaced using the IDEAS universal file format. Plots of results were acquired using MATLAB and WordPerfect. The pressure is calculated anywhere in the field for given velocity conditions on the boundaries. The calculated results are then compared with experiment using a novel technique for measuring throat impedance.

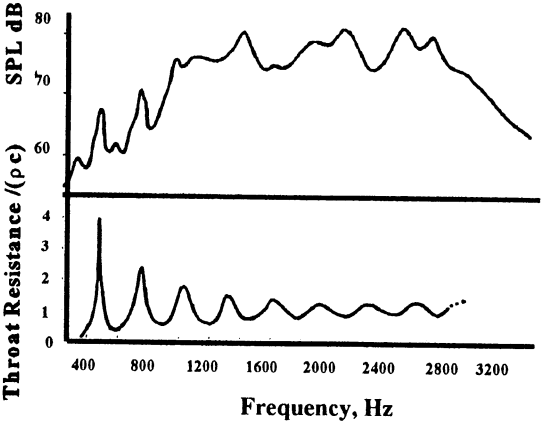

Figure 2 Disagreement between the radiated far-field sound and calculated throat impedance; figures from Edgar [6] following Olson.

2 THEORY

One seeks solutions of the scalar wave equation, which for sinusoidal variations of the pressure p and the velocity u reduces to the Helmholtz equation

$$\nabla^2 p + k^2 p = 0 \qquad (1)$$

with Neumann type boundary conditions over the surfaces for the normal velocity component u_n. At the horn-driver boundary the velocity is taken as 0.1m/s while over the horn boundaries u_n=0. The theory of the Helmholtz method for solutions to equation 1 using the Gauss divergence theorem is well documented in the literature. Following this Helmholtz integral approach and with the free-space Green's function e^{ikR}/R where R is the distance between field point and source point, the integration involves integrals over the horn surfaces for $p(\vec{r})$ of the form

$$p(\vec{r}) = \frac{1}{4\pi}\int_S [p(\vec{r}_0)\frac{e^{ikR}}{R}(ik - R^{-1})\cos(\theta) - i\omega\rho_0 u_n(\vec{r}_0)\frac{e^{ikR}}{R}]dS \qquad (2)$$

There is an "apparent" singularity when source and field points coincide, ie $R \to 0$, but can be removed by further subdivision of the source element and numerical integration, see Koopman and Benner [8]. There is also the Sommerfeld boundary condition at infinity, namely that $p \to 0$, $u \to 0$ as $r \to \infty$. There are no exact solutions for $p(\vec{r})$ for finite horns and so the problem lends itself to BEM computation. A great benefit of this approach is that the condition at infinity will automatically be satisfied.

The important physical interpretation of equation 2 that is required here is that the real horn surface can be removed and replaced by a monopole distribution with strengths proportional to $u_n(\vec{r}_0)$ and a dipole distribution with strengths proportional to $p(\vec{r}_0)$. Normally in a BEM acoustic problem the boundaries can be discretized into elements using no less than six elements per smallest acoustic wavelength over the surface. Here, the boundary thickness is effectively replaced by two separate distributions of sources and dipoles some distance t apart for studying the horn. It follows that the source and dipole distributions on the inner and outer surfaces of the horn sides cannot adequately describe the true surface, ie the interactions between the two sets of distributions, unless the element size is of order equal or less than the horn wall thickness t, see later.

3 MODEL

The three-dimensional geometrical description of the Klipsch K400 horn comprised two models. One model had a square throat of dimension 0.0157m and rectangular mouth exit of width 0.4223m, height 0.1448m, length 0.5366m, and exponential flares in width y_1 and height y_2 along length x, described by

$$y_1 = 0.00785e^{(6.135x)} \quad \text{and} \quad y_2 = 0.00785e^{(4.1403x)} \qquad (3)$$

By symmetry about axis x, only one-quarter of the three-dimensional geometry was required. The second model was of the same shape with the addition of a

baffle extending in width 0.7842m and in height 0.2476m at the exit, see Figure 3.

These two BEM models were then constructed with 6mm and 10mm horn wall thicknesses and nominal 6mm and 10mm element sizes, which resulted in two models with 977 and 2561 elements respectively. The larger model ran in 75 minutes per frequency or 151 hours for 121 frequencies over the frequency range 200-2KHz. This range was of the greatest interest for this K400 horn which had a design frequency range of 400-4KHz. The stringent monopole / dipole distribution representation arising from the modelling of the two surface boundaries meant that a larger model would not run in memory.

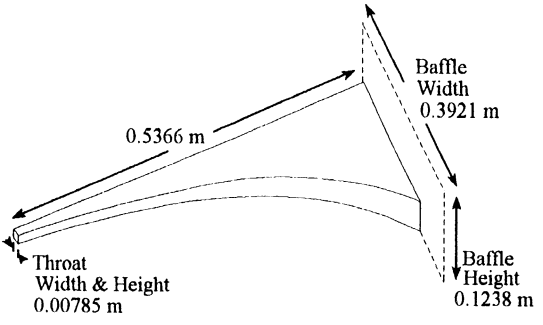

Figure 3 Quarter geometry for 3 dim. exponential horn geometry, without baffle and with baffle (dotted). The horn is symmetrical with respect to height and width dimensions shown.

4 COMPUTATIONAL RESULTS

The calculated real throat impedance for the finite K400 exponential horn using the Olson analytical approach, with the exit area modelled as terminating in an infinite baffle and using the Struve function development previously mentioned due to Sauter and Soroka, is shown by the solid-line of Figure 4.

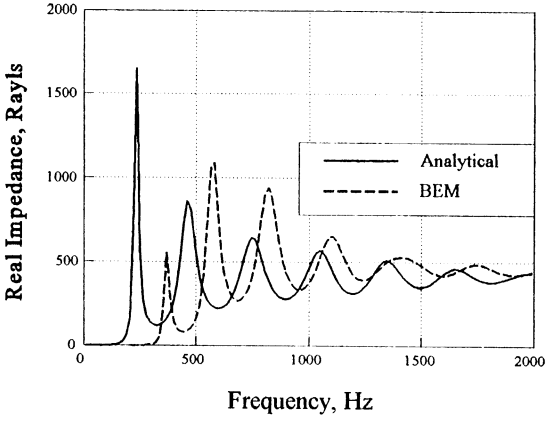

Figure 4 Real impedance in throat for 3 dim. exponential horn, analytical result for infinite baffle case and BEM result without baffle.

Unlike the infinite horn of Figure 1, the real impedance now has oscillations in amplitude due to the standing-wave patterns inside the horn due to reflection from the exit. Also plotted is the BEM analysis from the 977 element model without baffle. The incorrect assumption of an infinite baffle at exit, ignoring diffraction effects, causes the peaks in the impedance to be moved much lower in frequency.

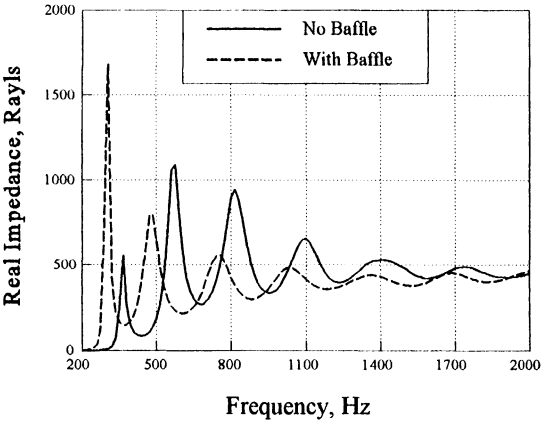

Figure 5 Real impedance in throat for 3 dim. exponential horn, with and without baffle.

The BEM computed results for the 2561 element model with the finite baffle of Figure 3 are plotted in Figure 5 together with the no-baffle BEM results from Figure 4. Again the effects of the finite baffle are to lower the frequencies of the impedance peaks.

The magnitudes of the throat pressure and far-field pressure at r=3m from the throat are plotted in Figure 6. The horn action is easily seen, since the throat pressure is of order 125dB SPL and has the lower value of 78dB SPL in the far-field (the air impedance was 415 Rayls in both cases). Note that the pressure peaks in the throat occur at the same frequencies as in the far-field.

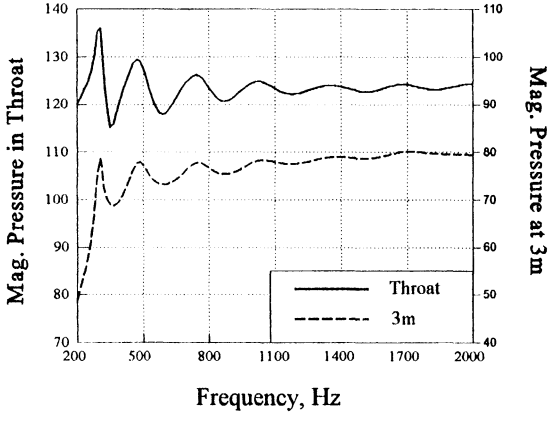

Figure 6 Magnitude of pressure in throat and at 3 meters for 3 dim. exponential horn, with finite baffle, dB re $2x10^{-5}$ Pa.

Of even

greater interest, related to the previous comments in the introduction for the impetus of this research, Figure 7 shows the BEM computed pressure at r=3m compared with the real impedance at the throat. There is no doubt that the frequencies of the peaks coincide! An innovative experiment was now performed to try to confirm these computed results.

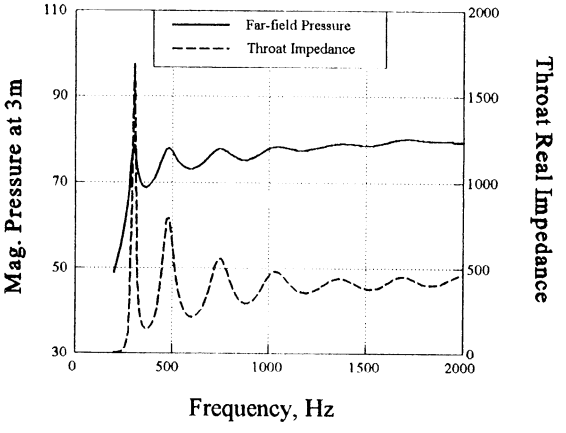

Figure 7 Three-dim. exponential horn with finite baffle, magnitude pressure at 3m, dB re $2x10^{-5}$ Pa, and throat impedance, Rayls.

5 EXPERIMENTAL MEASUREMENTS

Although there have been measurements of the throat impedance in a finite horn made by the standing-wave tube technique, see reference [3], there would appear to be no measurements in the literature which attempt to correlate the far-field pressure with the throat impedance.

An innovative method of measuring the diaphragm motion was to use the fiber-optic displacement detector first described by Cook and Hamm [9], and later used by Boone and Hodgson [10]. A photo-diode illuminates a central illuminating fiber, while six surrounding fibers which detect the reflected light from the surface, are connected to a photo-detector diode. The output signal is then amplified to produce a voltage signal proportional to displacement. The displacement detector has a resolution of order 10^{-5} mm with a linear operating range of 2.5mm.

The electro-magnetic driver chosen for the experiments was a University Sound Type 1828C with a samarium ceramic magnet and used a 38mm diameter phenolic diaphragm. The driver, see Figure 8, has standard pipe threads on both the front and the rear of the driver. This allowed a special fitting to be attached to the rear to locate the fiber-optic probe. A Bruel and Kjaer 3.18mm dia. type 4138 microphone was mounted in a screwed piece into the side of the throat in order to measure the throat pressure.

The driver and horn were excited using a solid-state power amplifier with random noise as input over the frequency band 100Hz to 10KHz. The horn was mounted on a tripod positioned outdoors on a platform 7m above the ground with horn axis horizontal. The far-field microphone was a Bruel and

Kjaer 12.7mm dia. type 4134 and was mounted at grazing incidence for flat frequency response at a distance of 1.5m from the throat, i.e. 1m from the exit on axis.

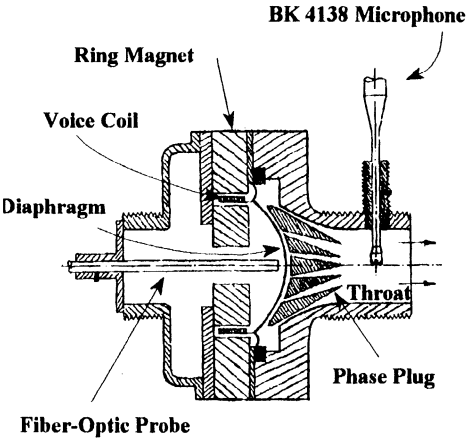

Figure 8 Cross-section through compression horn driver, University Sound Type 1828C (not to scale).

Spectral analyses were made of the throat pressure and velocity (after differentiation of the displacement signal), as well as for the far-field pressure, using a Hewlett-Packard Type 3562A FFT two-channel analyzer. In addition, the throat impedance, i.e. pressure divided by velocity, was also measured as a function of frequency using the arithmetic capability of the HP analyzer.

The measured throat impedance magnitude is plotted in Figure 9 which also shows the frequencies of the main impedance peaks. A measurement of the phase angle between the throat pressure and diaphragm velocity is plotted in Figure 10 and shows clearly that at low frequencies of order 250Hz, the phase tends to the reactive value of -90 degrees where the motion below cut-off is totally reactive. At higher frequencies, such as 2KHz, the phase does tend to order zero degrees. Because the throat pressure is measured 1.27cm in front of the diaphragm, their is a linear phase change with frequency due to time delay having value 26.7° at 2KHz. This time delay was corrected for by using the HP analyzer's programmable software. Also it is expected that there will be some reactance effect due to the sealed back chamber of the driver which will show up as

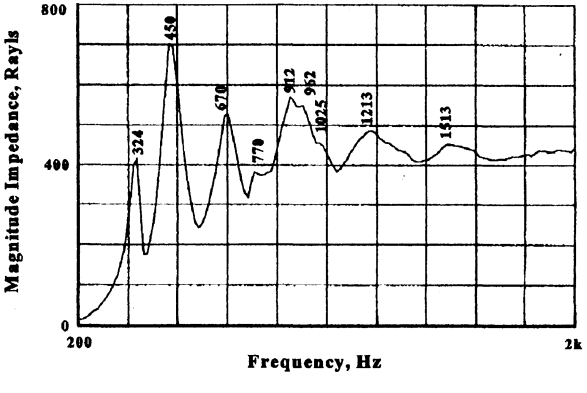

Figure 9 Throat impedance magnitude, showing frequencies of the dominant peaks.

some phase difference over the efficient frequency range of the driver. Further investigation of compression drivers is needed. Measurements of the throat pressure and velocity spectra were also taken together with the far-field spectra, but are not shown here.

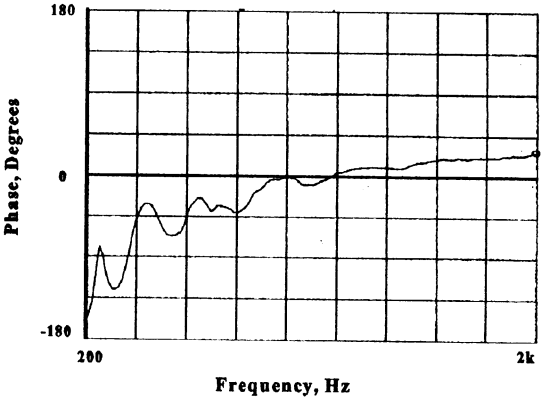

Figure 10 Throat impedance, phase.

The correspondence between the frequencies of the BEM calculated throat impedance peaks as compared with the measured throat impedance, pressure, velocity and far-field pressure are shown in Table 1.

Table 1 Comparison of frequency peaks in BEM and measured spectra.

Z-throat BEM	Z-throat Measured	p-throat Measured	u-throat Measured	p-farfield Measured	Comments
305	324	300	300	325	1
			387	390	
478	450	425		425	1
			580		
	670	670		650	2
747	770	737	737	750	1
		875			
	912				3
	962	975		950	2
1032	1025			1032	1

1 = Agreement between BEM and measured data
2 = Probable driver resonance
3 = Lateral standing wave

6 CONCLUSIONS

From Table 1, it would appear that the BEM computations of the acoustic impedance vs frequency for a finite exponential horn, such as the K400 horn with a finite baffle, correlate well with the frequencies of the measured peaks in the

throat impedance as well as with the far-field pressure for the first four BEM computed peaks, provided the experiments are conducted in an anechoic environment. However there are still some discrepancies which could be accounted for by lateral standing waves in the horn at higher frequencies or non-piston motion of the horn driver. Although not shown here, the measured far-field response had amplitude ripples of order +/-4dB in the worst case at low frequencies. Further investigation of driver performance is required.

REFERENCES

1. Lord Rayleigh, Theory of Sound, Macmillan, London, 1878.

2. Webster, A.G., "Acoustical Impedance, and the Theory of Horns and of the Phonograph," J. Audio Eng. Soc., Vol. 25, No. 1/2, Jan/Feb 1977 (Reprint of 1919 article).

3. Holland, K.R., Fahy, F.J., and Morfey, C.L., "Prediction and Measurement of the One-Parameter Behavior of Horns," J. Audio Eng. Soc., Vol. 39, No. 5, 1991.

4. Olson, H.F., Elements of Acoustical Engineering, Van Nostrand, 1940.

5. Sauter, A. and Soroka, W., "Sound Transmission through Rectangular Slots of Finite Depth between Reverberant Rooms," J. Acous. Soc. Am., Vol. 47, No. 1, 1970.

6. Underwood, R.L., "Re-examination of Acoustic Horn Theory by the Boundary Element Method and by Experiment," Ph.D. Thesis, Mechanical and Aerospace Engineering Department, NC State University, 1996.

7. Edgar, B.C., "The Edgar Midrange Horn," Speaker Builder, January 1986.

8. Koopman, G.H. and Benner, H., "Method for Computing the Sound Power of Machines Based on the Helmholtz Integral," J. Acous. Soc. Am., Vol.71, No.l, 1982.

9. Cook, R.O. and Hamm, C.W., "Fiber Optic Lever Displacement Transducer," Applied Optics, Vol.18, No.19, October 1979.

10. Boone, D.E. and Hodgson, T.H., "Surface Intensity Measurements Using a Fiber Optic-Pressure Probe," Proceedings of the International Congress on Recent Developments in Acoustic Intensity Measurement, Senlis, France, 1981.